American Journal of Materials Science 2026, 16(1): 19-26
DOI: 10.5923/j.materials.20261601.03

Green Method, Influence of pH on Optical Properties and Particle Size for Biosynthesis of ZnO Nanoparticles Using *Strychnos henningsii* Leaves Extracts

Lucy J. Chebor[1,*], Lusweti Kituyi[1], Dickson Andala[2], Kiplagat Ayabei[1]

[1]Department of Chemistry & Biochemistry, University of Eldoret, Eldoret, Kenya
[2]Department of Chemistry Multimedia University, Nairobi, Kenya

Abstract The green synthesis of zinc oxide nanoparticles (ZnO NPs) using plant-derived extracts has attracted considerable scientific interest owing to its environmentally sustainable nature, operational simplicity, and cost-effectiveness. In this study, ZnO NPs have been synthesized and characterized from *Strychnos henningsii leaf* extract as a bio-reducing and stabilizing agent. The synthesis was carried out at 70 ℃ across a pH range of 5–9 to examine the influence of reaction conditions on the structural and optical properties of the resulting nanoparticles. The structural and optical characteristics of the nanoparticles were examined systematically. X-ray diffraction (XRD) analysis confirmed the formation of a single-phase hexagonal wurtzite ZnO structure. Optimal crystallinity was achieved at pH 8, with a crystallite size of approximately 16.22 nm, accompanied by minimal lattice strain and low dislocation density. Optical analysis by Ultra Violet-Visible spectrum showed sharp edges of absorption with a band gap of 3.37 eV at pH 8, and photoluminescence (PL) analysis showed minimal defect emissions at pH 8. However, at lower pH values (5-6), larger defect-containing nanoparticles with increased lattice parameters were obtained, and at higher pH (9), aggregation and low optical quality were observed. Generally, the predominant pH (8) yielded the most crystalline, defect-minimized, and optical active nanomaterials of the ZnO nanoparticles. These results offer a sustainable plant-based pathway towards modification of the ZnO nanoparticles to be applied in nanotechnology.

Keywords Nanotechnology, Single phase, Green synthesis, Quantum, Optical, Lattice strain

1. Introduction

Nanotechnology is an innovative and rapidly advancing field that involves the design and fabrication of novel materials at the nanometer scale. When compared with materials that have an undefined particle size, nanomaterials consist of small particles with a large specific surface area, resulting in materials that display unexpected surface area, volume, quantum size, and macro tunnelling effects. Nanomaterials exhibit unique optical, mechanical, catalytic, and biological properties, which contribute to their wide range of potential applications [1].

Nanomaterials and nanotechnologies are raising significant hopes because of the specific properties of matter at the nanometric scale, which make it possible to envisage new functions that were unimaginable until now [2]. Zinc oxide nanoparticles (ZnO NPs) are notable among them, with great interest due to their unique properties. ZnO is a non-toxic multifunctional inorganic material with a wide range of uses in several fields such as photovoltaic, electronics and drug delivery [3]. ZnO is a wurtzite-type light electronic and photonic semiconductor with a high exciton binding energy (60 me V) at room temperature and a large direct bandgap of 3.37 eV [4]. The strong binding energy of ZnO excitons allowed excitonic evolutions even at room temperature.

Metal oxide nanoparticles are one of several types of nanomaterials that have gained considerable interest because of the distinctive optical, chemical, and physical traits separating them from their counterparts in bulk (high surface-to-volume ratio, increased reactivity, quantum confinement effects), among others [5]. ZnO nanoparticles are among the most investigated metal oxides; this aspect is mainly because of their multifunctional capacity. ZnO is an ultraviolet (UV) wide-bandgap (3.37eV) semiconductor that has a substantial exciton binding energy, biocompatibility, and photocatalytic and antimicrobial potential, as well as the ability to be applied in environmental protection, sensor and drug delivery, and optoelectronic applications [4]. The physicochemical properties of ZnO nanoparticles, including size, morphology, and crystallinity, are strongly influenced by synthesis parameters such as pH, temperature, and reaction

* Corresponding author:
lucychebor@yahoo.com (Lucy J. Chebor)
Received: Mar. 9, 2026; Accepted: Apr. 3, 2026; Published: Apr. 20, 2026
Published online at http://journal.sapub.org/materials

time [3]. It is thus important in the process of synthesis to fine-tune responses to such conditions to get the desired functional performance in specific applications. Although these conventional techniques of chemical synthesis such as sol-gel, co-precipitation, and hydrothermal techniques, are effective, they use toxic solvents, expensive set-ups, and harsh reaction conditions, which render them hazardous on a broader level, to both the environment and the health of the workers [6]. Alternatively, in green synthesis, plant extracts has provided a solution with the utilization of natural phytochemicals as reducing and capping agents. The method is environmentally sustainable, economically viable, scalable, and eliminates the need for hazardous reagents [7]. The production of the nanoparticles with the help of the plants is promoted by an abundance of secondary metabolites, including flavonoids, phenols, alkaloids, and terpenoids that can be characterized as the natural chelating and stabilizing agents [6]. Specifically, leaf extracts have shown great efficiency in yielding metal oxide nanoparticles in a stable and uniform distribution [8]. In this regard, the *Strychnos henningsii*, is an indigenous African medicinal plant, belonging to the Loganiaceae family. The species offers significant potential for green nanoparticle synthesis due to its bioactive constituents. Notably, it is abundant in alkaloids and has a long history of traditional use for managing gastrointestinal ailments, rheumatism, and microbial infections [9]. However, it is yet to be utilized in the production of nanoparticles even though it has a lot of ethnobotanical significance.

This study presents an efficient and sustainable strategy for biosynthesizing ZnO NPs from Zinc Nitrate dihydrate ($Zn(NO_3)_2.2H_2O$) solution using *strychnos henningsii* leaves extract as a reducing agent. To the best of our knowledge, this is the first study that looked at the effects of pH values of 5, 6, 7, and 8 on ZnO NP production, optical properties, and crystal size. Nevertheless, there is a scarcity of detailed works examining the effects that this parameter has on the properties of ZnO nanoparticles, especially when the latter are made through *Strychnos henningsii*.

2. Experimental Procedure

Preparation of *S. heningsii leaf* extract

Leaves of *Strychnos heningsii* plant were collected, taken to the laboratory, carefully sorted, washed using both tap and distilled water, air-dried at room temperature for two weeks until completely dry then finely ground to powder using a blender. A 10 g powdered material was transferred to 200 ml of boiling distilled water in a borosilicate beaker and stirred using a magnetic stirrer for a duration of one hour, until the solution turned brown. Filtration of the mixture using Whatman filter paper (No.1) gave a clear solution, which was stored for the synthesis of ZnO and TiO_2 nanoparticles.

Green Synthesis of Zinc oxide Nanoparticles

A 50 ml solution of 0.1 M zinc nitrate was made by dissolving zinc nitrate in deionized water and stirred using magnetic stirrer for a period of 5 minutes. The zinc nitrate solution was heated and blended with 30 ml of plant extract while maintaining continuous stirring to form a dark brown solution. A 0.5 M NaOH and 0.1M HNO_3 solutions were used to adjust the pH (5, 6, 7, 8 and 9). Heating this amalgam of solutions at a constant temperature of 70 ℃ for a duration of 2 hours, with rigorous stirring throughout the process resulted in pale yellow solution, confirming the ZnO nanoparticles formation. Centrifugation at 7000 rpm for 15 minutes removed the precipitate, which eventually underwent a transformation from brown to a solid pale-yellow colour. Subsequently, purification was carried out by sequential washing with de-ionized water, followed by oven drying, then the dried material was annealed at 500 degrees for two hours to remove impurities, mashed in a ceramic mortar pestle to get a finer nature for characterization purposes. Ultimately, this process yielded a final product in the form of white-coloured powder.

3. Results and Discussion

FTIR Analysis

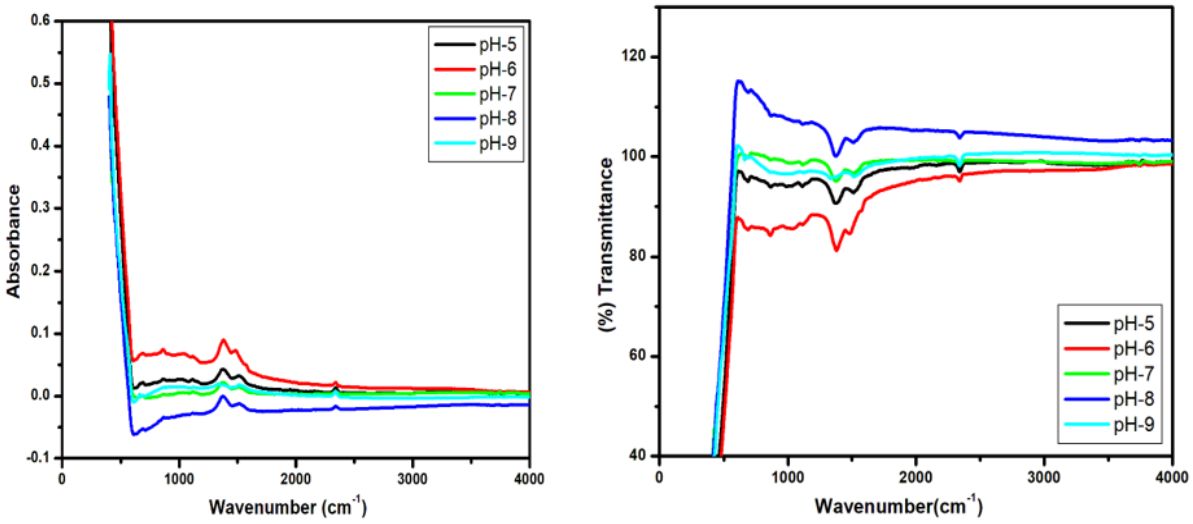

Figure 1. FTIR absorbance spectra of synthesized samples

The Fourier Transform Infrared (FTIR) spectroscopy was used to determine the functional groups present on the surface of the produced ZnO nanoparticles and establish whether phytochemicals in *Strychnos henningsii* leaf extract were involved in the nanoparticle formation process or not. FTIR spectra of nanoparticles of ZnO precipitated at different pH (5-9) at a constant temperature of 70 ℃ are shown in Fig. 1a (absorbance) and Fig. 1b (transmittance), respectively.

In all spectra, there was a strong, prominent absorption band with a lower wavenumber range of 400 and 600 cm^{-1}, characteristic of the ZnO stretching motion and an indication that the formation of ZnO nanoparticles was successful [10]. This ZnO band was strongest at pH 6, which suggests that at this pH, nanoparticle formation or crystallinity was higher. The same pattern occurred with green-synthesized NPs of ZnO using *Moringa oleifera* and *Azadirachta indica*, wherein intense ZnO vibrations were obtained here [11].

The O-H stretching vibration of the hydroxyl structure correspond to broad absorption bands between 3200 and 3500 cm^{-1} commonly found in residual water molecules or phenolic compounds of a plant extract [12]. These were even greater at lower pH, particularly at pH 5 and 6, meaning that there was greater retention of polar phytochemicals in the acid environment. Moderate and low peaks at 1600 to 1700 $cm^{-1,}$ depicted stretching vibrations of the C=O bonds of the carbonyl functions of flavonoids and alkaloids present in *Strychnos henningsii* extract [13]. These peaks became weaker with increased pH, suggesting that alkalinity could suppress the availability or the activity of some of the bioactive molecules within the reaction medium. Absorptions at 1400 to 1450 cm^{-1} could be attributed to C-N stretching vibration of amines or potential symmetric stretching of -COO- functional groups, indicating that amino acids or proteins participated in the reduction and stabilization of nanoparticles [14]. Stability in these groups has often been reported to occur due to capping of ZnO nanoparticles by these groups, which avoids agglomeration. Furthermore, a weak band at 1050 to 1100 cm^{-1}, which was prominent at pH 6 and 7, could be attributed to stretching vibrations of C-O in the alcohols or ethers, confirming the role of phytochemical compounds in the nanoparticle structure [15]. The spectra of transmittance were complementary, and low transmittance (at pH 6, especially in the Zn-O and O-H zones) indicated higher absorbance, further indicating that this pH supports efficient synthesis of these nanoparticles and subsequent optimal contact with the biomolecules. These observations prove that the pH has a tremendous effect on the surface chemistry and organic functional group attachment in the formation of ZnO nanoparticles using green synthesis. Such patterns in pH-dependent FTIR shifts have also been described in other works using ZnO nanoparticle preparations produced via Ocimum sanctum [16] and *Carica papaya* leaf extract [17], continuing to support these findings. In such studies, more specific ZnO peaks were found to exhibit high interactions with capping phytochemicals in an acidic to neutral pH range.

Optical Analysis

An eco-friendly, plant-mediated method for obtaining ZnO NPs has the advantage of utilizing phytochemicals (alkaloids, phenolics, terpenoids) as both bioreductants and capping agents. This aligns with the literature on the green synthesis of metal oxide nanomaterials, which focuses on economical and scalable synthesis [18]. Optically, ZnO nanoparticles exhibit a direct wide band gap of 3.37 eV and an exciton binding energy of 60 meV. When prepared as high-quality particles, they show a sharp UV band-edge at 360–380 nm with minimal absorption in the visible range [19]. In plant-mediated systems, the pH of the solution is the control that adjusts hydrolysis, growth, and surface defect chemistry, hence the sharpness of the edge and any sub-gap visible tailing [20].

The figure below shows the absorbance spectra of synthesized ZnO nanoparticles at different pH levels.

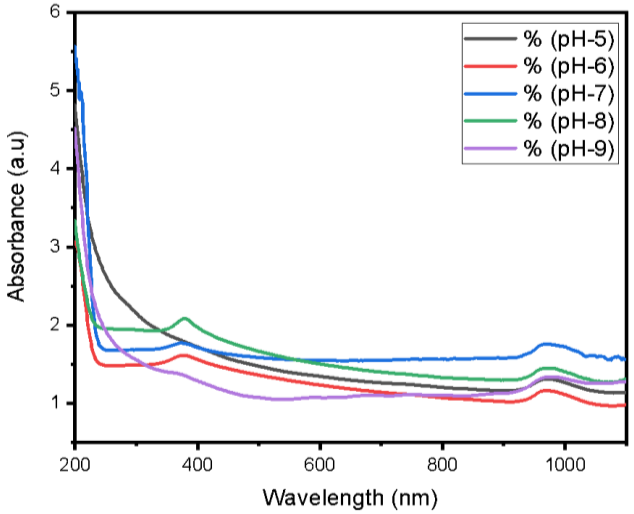

Figure 2. UV -Vis Absorbance of the synthesize

As shown in Figure 2, the sample synthesized at pH 8 exhibits the sharpest UV band edge and the weakest visible-range baseline, indicating the fewest deep defect states. The sample at pH 7 displays a similar optical profile. This behavior can be attributed to a more balanced OH environment, which favors controlled nucleation and efficient phytochemical capping, leading to well-ordered crystallites with reduced sub-gap absorbers [20]. In contrast, pH 9 performs as a mild outlier, and the presence of pH closer to (9.7) lowers the electrostatic repulsion and promotes aggregation, which softens the edge and introduces a defect-mediated absorption despite a sufficient OH [21]. The pH of 5 demonstrates the poorest optical quality, with a strong visible tail characteristic of a defect rich environment and the presence of residual organics.

The Tauc plot in Figure 3 shows the observed band gaps, 3.37 eV (pH 8), 3.52 eV (pH 7), 3.68 eV (pH 9), 4.00 eV (pH 6), and 5.50 eV (pH 5). The pH 8 value (3.37 eV) is equivalent to the reported value of the typical band gap of zinc oxide (3.3 eV) and the range of UV-edge in green ZnO (3.2-3.4 eV, 355-380 nm) [21]. At pH 7 (3.52 eV), a slight

blue shift was observed, which could be attributed to filling of shallow donor states and with less tailing of a cleaner edge.

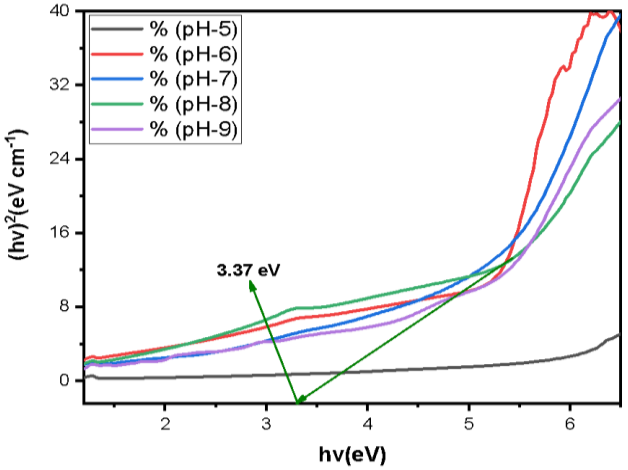

Figure 3. Tauc plot for extrapolated band gaps of synthesized ZnO NPs at of pH 5 to 9

At pH 9 (3.68 eV), it is further blue-shifted but with a softer edge attributed to both aggregations induced by scattering near the isoelectric point as well as donor-like defects. However, at the pH of 6 (4.00 eV) and pH 5 (5.50 eV) are higher than physically expected of ZnO in plant-mediated dispersions, inflated Tauc intercepts are possible when the edge region is weak, when diffuse-absorbance models are mismatched, or when defect tailing distorts linear fits. More methodological studies recently provide cautionary notes that the Tauc extrapolations of polycrystalline material may overestimate Eg unless the true linear regime is strictly defined [22]. Therefore, as much as the trend (Eg, at pH 8 somewhat bulk, pH 7 a little larger, pH 9 anomalous; pH 5-6 unreliable) is significantly informative, the absolute Eg at pH 5-6 might be better considered as counterfeit rather than real broadening of the ZnO gap.

The optimal pH-8 is explained by the combination of OH-driven hydrolysis and phytochemicals within *Strychnos henningsii* that cap emerging nuclei, suppress surface states, and result in a typical ZnO edge. pH 7 behaves the same, with slightly different defect populations. pH 9 no longer performs well because neutralization near the isoelectric point encourages immobilization and disrupts the edge despite reasonable hydroxide availability. pH 5 undermines itself due to ineffective hydrolysis. This pH-dependent optical fingerprint is consistent with recent green ZnO studies of the sharpest UV spectra and most plausible Eg, and extreme pH conditions bias defects or aggregation [22].

The systematic investigation of pH 5-9 in Strychnos *henningsii* catalyzed ZnO and confirmation that pH 8 offers the best optical quality with clean edge, bulk-like Eg offers plant-specific data that are largely absent in the recent green-ZnO literature, which tends either to report just a single pH of synthesis or not explicitly connect pH to the visible suppression and credible Tauc analysis. This could be attributed to the purity of a single *Strycnos henningsii* with a distinct phytochemical profile, with controlled pH and spectra comparable with the most stringent reports on green-ZnO band-edge characterization [23]. The band gap values are shown in Table 1.

Table 1. Extrapolated band gap values of synthesized ZnO NPs at different pH levels

Ph	Band Gap (eV)
5	5.50
6	4.0
7	3.52
8	3.37
9	3.68

XRD Analysis

All XRD patterns show hexagonal structures of wurtzite ZnO and match the JCPDS card 01-070-8072 with planes (100), (002), (101), (102), (110), (103), (200), showing ZnO in only a single phase using Strychinos *henningsii* as a plant-mediated green synthesis procedure and phytochemical capping agent. This matches with recent publications of wurtzite ZnO synthesized under plant extracts, confirming that the pH only modulates microstructure and not the phase. The XRD pattern is shown in Figure 4.

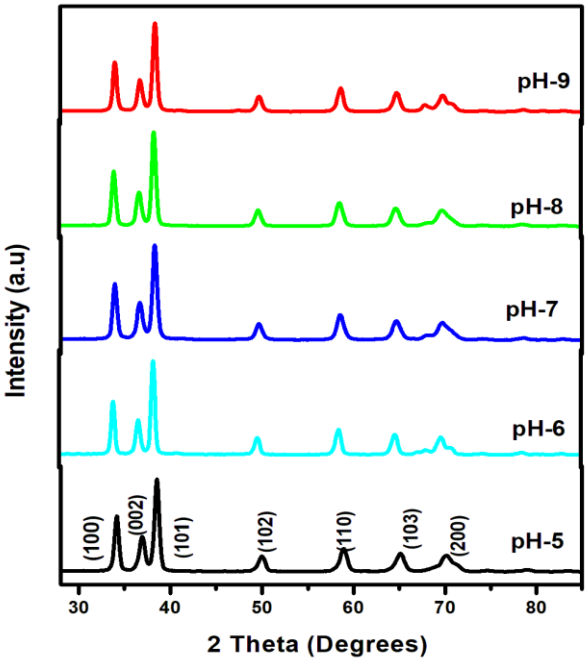

Figure 4. XRD pattern of synthesized samples at different levels of pH

The main diffraction peak shifted toward a higher 2θ value at pH 8 (38.52 °), corresponding to the smallest d-spacing (0.2334 nm) and the lowest lattice parameters *a* and *c* (0.3064 and 0.4909 nm, respectively). According to Bragg's law, such a shift toward higher 2θ indicates lattice contraction, reflected by reduced interplanar spacing and improved crystal packing. This suggests the formation of a more compact

inorganic framework at pH 8, likely resulting from enhanced hydrolysis and balanced OH^- availability together with effective phytochemical capping under near-neutral to slightly alkaline conditions [3]. A slight increase in d-spacing was observed at pH 9 (0.2345 nm). This behavior is associated with nanoparticle aggregation near the isoelectric point of ZnO (≈8.7), which can disrupt lattice packing and result in anomalous structural behavior at higher pH.

When the pH increase, the FWHM increased, and crystallite size (D) calculated from the Scherrer equation decreased. The pH of 8 (FWHM 0.00737, 0.00906 radians, D 19.92 to 16.22 nm), with pH 7 similar to pH 8 (D = 16.57 nm) as shown in Table 3. This is the standard size broadening behaviour, and the associated increase in dislocation at lower D indicates finite-size line broadening effects rather than secondary phases [24]. Scherrer analysis suggests that decreasing crystallite size (D) is typically accompanied by increased microstrain and dislocation density, which may influence the structural quality of the material. Nevertheless, the synthesized ZnO exhibited well-defined nanocrystals with an average size of ~16 nm, indicating an optimal balance between crystallite size, reduced lattice strain, and low dislocation density, together with a slight shift toward higher 2θ values [25].

Table 2. 2θ, FWHM and crystallite size of ZnO NPs with pH values

pH	2θ	FWHM	FWHM (Radians)	Crystallite size D (nm)
5	38.26	0.4220	0.007365	19.92
6	38.36	0.4735	0.008264	17.76
7	38.31	0.5075	0.008857	16.57
8	38.52	0.5188	0.009055	16.22
9	38.33	0.4659	0.008132	18.05

Table 3. Crystallite size, strain, and dislocation densities of synthesized materials with pH

pH	2θ (°)	Crystallite size D (nm)	Strain	Dislocation density (nm^{-2})
5	38.26	19.92	0.005307	0.002518
6	38.36	17.76	0.005939	0.003169
7	38.31	16.57	0.006373	0.003641
8	38.52	16.22	0.006477	0.003800
9	38.33	18.05	0.005848	0.003069

From Figure 4 and Tables 2 and 3, the overall structural quality was better at pH 8, followed by pH 7, pH 6, pH 9 (outlier), and pH 5. At pH 8, the (101) diffraction peak appeared at the highest 2θ value (38.52 °), corresponding to the smallest d-spacing (0.2334 nm) and the lowest lattice parameters *a* and *c* (0.3064 and 0.4909 nm, respectively). The crystallite size remained relatively small (16.22 nm), which may be attributed to an optimal balance between OH^- availability and phytochemical capping, promoting efficient condensation and tighter lattice packing.

The sample synthesized at pH 7 exhibited similar structural characteristics. In contrast, the sample at pH 5 showed a lower 2θ value (38.26 °), the largest d-spacing (0.2350 nm), and the highest lattice parameters (a = 0.3084 nm, c = 0.4942 nm), together with a larger crystallite size (19.92 nm). Despite the larger Scherrer size, the expanded lattice and looser packing at pH 5 may result from incomplete hydrolysis and the presence of residual organic species under acidic conditions. This behavior is consistent with the poorer optical quality observed at this pH.

Photoluminescence Analysis

The photoluminescence (PL) of ZnO NPs synthesized with Strychnos *henningsii* leaf extract contains important information about the defect chemistry and surface states of the nanoparticles. Emission peaks in the blue-green wavelength (437-492 nm) indicate defect-induced emissions regarding oxygen vacancies (V_O) and zinc interstitials (Zni), which are radiative recombination centres [26]. Phytochemicals in S. *henningsii* (alkaloids, phenolics, and terpenoids) are probable reducing agents in the synthesis of nanoparticles and stabilizing agents that aid in controlling nanoparticle size and surface properties [16].

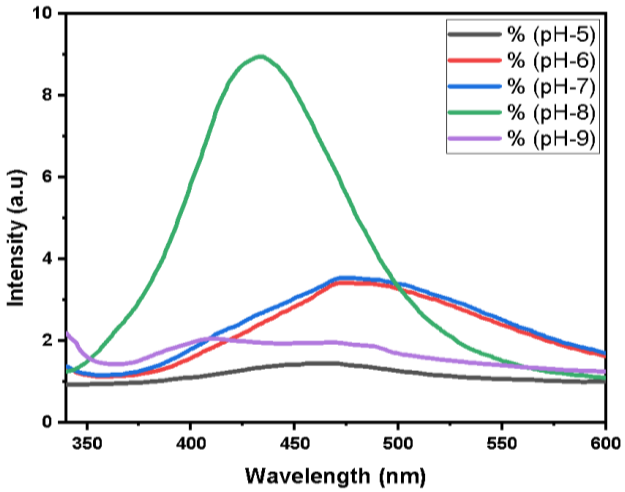

Figure 5. photoluminescence spectra of synthesized sample at pH 5-9

Figure 5 shows the PL spectral shifts to the emission peaks across different pH values and the highest emission of 437 nm occurred at pH 8 with a peak of 7.49 a.u.

The emission is generally attributed to zinc interstitials (Zni) and oxygen vacancies (V_O), which are typical of defect-prone ZnO nanoparticles [27,28]. The peak showed the highest intensity among all pH conditions, indicating reduced defect states and improved crystallinity of the synthesized ZnO at pH 8. This observation is consistent with the XRD and UV–Vis analyses, which similarly reveal enhanced crystallinity and sharper optical band edges at this pH [29]. At pH 5, the peak emission shifted to 464 nm at a low intensity of 0.46 a.u., a higher defect density than at pH 8. This is consistent with the findings of UV-Vis, whereby the strongest visible absorption tail was observed at pH 5, implying the presence of more defects and surface states [30].

Table 4. Crystallite size, intensity, d-spacing and lattice parameters of synthesized materials for pH 5-9

pH	2θ	FWHM (Radians)	Intensity a.u.	d-spacing nm	Lattice parameters a	c
5	38.26	0.007365	1918.4	0.2350	0.3084	0.4942
6	38.36	0.008264	2113.0	0.2344	0.3077	0.4929
7	38.31	0.008857	1692.1	0.2347	0.3080	0.4935
8	38.52	0.009055	1838.8	0.2334	0.3064	0.4909
9	38.33	0.008132	1796.6	0.2345	0.3079	0.4933

The lowest photoluminescence (PL) intensity was recorded at pH 8, followed by pH 7 (2.52 a.u.) and pH 6 (2.32 a.u.). This behavior indicates that higher pH conditions favor improved crystallinity and reduced defect density in ZnO nanoparticles, leading to fewer radiative recombination centers. Therefore, the diminished PL intensity at pH 8 reflects the lower defect concentration and enhanced structural quality of the synthesized ZnO [27]. Conversely, at pH 9, the PL intensity was the lowest (0.77 a.u.), and the emission peak shifted to 442 nm, indicating that aggregation around the isoelectric point (IEP) of the ZnO introduced defects back and destabilized the crystal structure, leading to a decrease in optical quality. This agrees with the XRD and UV-Vis findings, which show worse crystallinity and more aggregation at pH 9 [16].

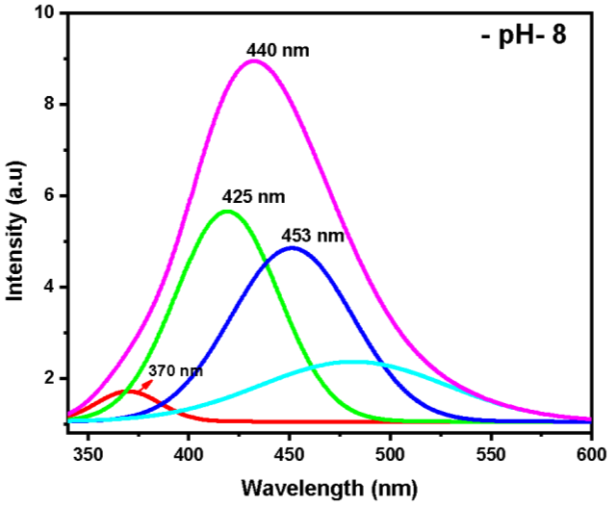

Figure 6. photoluminescence deconvolution of synthesized material at pH 8

At pH 8, the PL deconvolution in Figure 6 indicates various emission peaks at 370 nm, 425 nm, 440 nm, and 453 nm that are associated with various defect states within the lattice of ZnO. The peak located at 370 nm is associated with the presence of zinc interstitials (Zni), whereas the peaks at 425 and 453 nm are associated with oxygen vacancies (V_O) and complexes of oxygen vacancies, which serve as radiative recombination sites [3]. The highest intensity of the peak at 440 nm, where free exciton recombination occurred, was at pH 8, meaning minimal defects, and the most ordered crystal structure [27]. The PL deconvolution data also suggest that pH 8 generates the most crystalline and defect-free and is best suited to applications that involve efficient electron transfer, including photocatalysis and sensing [28].

Fresh information on the pH response of the nanoparticles of ZnO prepared through a green-synthesis process with the help of *Strychnos henningsii* leaf extract is provided. Table 5 shows emission wavelength and peak intensities of synthesized material at pH 5-9.

Table 5. Emission wavelength and Peak intensities of synthesized samples at different pH levels

pH	Emission wavelength (nm)	Peak Intensity (a.u)
5	464.15	0.46256
6	492.21	2.3224
7	490.26	2.5168
8	437.04	7.4877
9	442.14	0.76709

Through a systematic increase and decrease of pH between pH 5 to 9, it could be determined that pH 8 is the most favourable synthesis environment that can yield defect-free, highly crystalline, with an optimal optical property (both in PL and UV-Vis). Although past research has already been done on the role of pH in regulating defect density in green -synthesized ZnO, a distinctive feature of this work is the inclusion of *Strychnos henningsii* phytochemicals contribution and its impact on the PL emission. Results indicate, that pH 8 was not just the best value in terms of structural quality shown by XRD and UV-Vis but also the photocatalytic and sensing properties, as low defect density and high crystallinity are vital attributes that enable effective operation [29]. This pH-tuning approach is an eco-friendly solution to maximise the properties of ZnO without using harmful chemicals, which is a significant addition to the developing science of green nanotechnology [31,32].

4. Conclusions

This study successfully demonstrates the green synthesis of ZnO nanoparticles using the Strychnos *henningsii* leaf extract, where the phytochemicals of the extract can be used as both reducing and stabilizing agents. The methodical study of pHs varying between 5 and 9 showed that pH 8 is best, resulting in the most crystalline, the least number of defects, and the sharpest optical characteristics of the ZnO nanoparticles. Also highlighted are the importance of pH in regulating crystallite size, defect density, as well as optical band gaps, photoluminescence emission and structural order.

ACKNOWLEDGEMENTS

The authors are indebted to Murang'a and Egerton Universities for technical support.

Conflict of Interest

No conflict of interest.

REFERENCES

[1] Haleem, A., Javaid, M., Singh, R. P., Rab, S., & Suman, R. (2023). Applications of nanotechnology in medical field: a brief review. Global Health Journal, 7(2), 70-77.

[2] Afolalu, S. A., Ikumapayi, O. M., Oloyede, O. R., Ogedengbe, T. S., & Ogundipe, A. T. (2022). Advances in Nanotechnology and Nanoparticles in the 21st Century–an overview. Proceedings of the International Conference on Industrial Engineering and Operations Management. Nsukka, Nigeria,

[3] Aldeen, T. S., Mohamed, H. E. A., & Maaza, M. (2022). ZnO nanoparticles prepared via a green synthesis approach: Physical properties, photocatalytic and antibacterial activity. Journal of Physics and Chemistry of Solids, 160, 110313.

[4] Droepenu, E. K., Wee, B. S., Chin, S. F., Kok, K. Y., & Maligan, M. F. (2022). Zinc oxide nanoparticles synthesis methods and its effect on morphology: A review.

[5] Malik, S., Muhammad, K., & Waheed, Y. (2023). Nanotechnology: a revolution in modern industry. Molecules, 28(2), 661.

[6] Patil, N., Bhaskar, R., Vyavhare, V., Dhadge, R., Khaire, V., & Patil, Y. (2021). Overview on methods of synthesis of nanoparticles. International Journal of Current Pharmaceutical Research, 13(2), 11-16.

[7] Pulingam, T., Foroozandeh, P., Chuah, J.-A., & Sudesh, K. (2022). Exploring various techniques for the chemical and biological synthesis of polymeric nanoparticles. Nanomaterials, 12(3), 576.

[8] Latolla, N. S. (2022). Phytochemical Investigation and Antidiabetic Activity of Cissampelos capensis and Strychnos henningsii the Eastern Cape Medicinal Plants.

[9] Srujana, S., & Bhagat, D. (2022). Chemical-based synthesis of ZnO nanoparticles and their applications in agriculture. Nanotechnology for Environmental Engineering, 7(1), 269-275.

[10] Alharbi, F. N., Abaker, Z. M., & Makawi, S. Z. A. (2023). Phytochemical substances—mediated synthesis of zinc oxide nanoparticles (ZnO NPS). Inorganics, 11(8), 328.

[11] Radulescu, D.-M., Surdu, V.-A., Ficai, A., Ficai, D., Grumezescu, A.-M., & Andronescu, E. (2023). Green synthesis of metal and metal oxide nanoparticles: a review of the principles and biomedical applications. International Journal of Molecular Sciences, 24(20), 15397.

[12] Souza, T. A., Menezes, A. C., Santos, C. K., Jesus, F. G., Rocha, E. C., & Araújo, M. S. (2024). Toxicity of Bioactive Compounds of Strychnos pseudoquina (Loganiaceae) in Spodoptera frugiperda (Noctuidae). Sustainability, 16(11), 4430.

[13] Nair, G. M., Sajini, T., & Mathew, B. (2022). Advanced green approaches for metal and metal oxide nanoparticles synthesis and their environmental applications. Talanta Open, 5, 100080.

[14] Ismail, S. M. M., Ahmed, S. M., Abdulrahman, A. F., & AlMessiere, M. A. (2023). Characterization of green synthesized of ZnO nanoparticles by using pinus brutia leaves extracts. Journal of Molecular Structure, 1280, 135063.

[15] Karam, S. T., & Abdulrahman, A. F. (2022). Green synthesis and characterization of ZnO nanoparticles by using thyme plant leaf extract. Photonics,

[16] Abdelbaky, A. S., Abd El-Mageed, T. A., Babalghith, A. O., Selim, S., & Mohamed, A. M. (2022). Green synthesis and characterization of ZnO nanoparticles using Pelargonium odoratissimum (L.) aqueous leaf extract and their antioxidant, antibacterial and anti-inflammatory activities. Antioxidants, 11(8), 1444.

[17] Singh, S., Gade, J. V., Verma, D. K., Elyor, B., & Jain, B. (2024). Exploring ZnO nanoparticles: UV–visible analysis and different size estimation methods. Optical Materials, 152, 115422.

[18] Abdelghani, G. M., Ahmed, A. B., & Al-Zubaidi, A. B. (2022). Synthesis, characterization, and the influence of energy of irradiation on optical properties of ZnO nanostructures. Scientific Reports, 12(1), 20016.

[19] Indumathi, T., Theivarasu, C., Pradeep, I., Rani, M. T., Magesh, G., Rahale, C. S., & Kumar, E. R. (2021). Effects of Nd doping on structural, optical, morphological and surface-chemical state analysis of ZnO nanoparticles for antimicrobial and anticancer activities. Surfaces and Interfaces, 23, 101000.

[20] Ghosh, S., Ghosh, A., Pramanik, S., Kuiri, P. K., Sen, R., & Neogi, S. K. (2022). Synthesis of ZnO nanoparticles by co-precipitation technique and characterize the structural and optical properties of these nanoparticles. Journal of Physics: Conference Series,

[21] de Almeida, W. L., Ferreira, N. S., Rodembusch, F. S., & de Sousa, V. C. (2021). Study of structural and optical properties of ZnO nanoparticles synthesized by an eco-friendly tapioca-assisted route. Materials Chemistry and Physics, 258, 123926.

[22] Almarhoon, Z. M., Indumathi, T., & Kumar, E. R. (2022). Optimized green synthesis of ZnO nanoparticles: evaluation of structural, morphological, vibrational and optical properties. Journal of Materials Science: Materials in Electronics, 33(30), 23659-23672.

[23] Jayachandran, A., Aswathy, T., & Nair, A. S. (2021). Green synthesis and characterization of zinc oxide nanoparticles using Cayratia pedata leaf extract. Biochemistry and Biophysics Reports, 26, 100995.

[24] Sedefoglu, N. (2023). Characterization and photocatalytic activity of ZnO nanoparticles by green synthesis method. Optik, 288, 171217.

[25] Sarkar, T., Kundu, S., Ghorai, G., Sahoo, P. K., & Bhattacharjee, A. (2023). Structural, spectroscopic and morphology studies on green synthesized ZnO nanoparticles. Advances in Natural Sciences: Nanoscience and Nanotechnology, 14(3), 035001.

[26] Ramalingam, R., Sadasivuni, K., Allohedan, H., Sunderajan, M., & Yuvaraj, S. (2025). Photoluminescent, optical and magnetic property characterization of green chemistry method prepared calcium doped ZnO nanoparticles. Journal

of Ovonic Research, 21(1).

[27] Ramesh, P., Saravanan, K., Manogar, P., Johnson, J., Vinoth, E., & Mayakannan, M. (2021). Green synthesis and characterization of biocompatible zinc oxide nanoparticles and evaluation of its antibacterial potential. Sensing and Bio-Sensing Research, 31, 100399.

[28] Al-Harbi, H. F., Awad, M. A., Ortashi, K. M., Al-Humaid, L. A., Ibrahim, A. A., & Al-Huqail, A. A. (2025). Green Synthesis of Zinc Oxide Nanoparticles: Physicochemical Characterization, Photocatalytic Performance, and Evaluation of Their Impact on Seed Germination Parameters in Crops. Catalysts, 15(10), 924.

[29] Wijesinghe, U., Thiripuranathar, G., Iqbal, H., & Menaa, F. (2021). Biomimetic synthesis, characterization, and evaluation of fluorescence resonance energy transfer, photoluminescence, and photocatalytic activity of zinc oxide nanoparticles. Sustainability, 13(4), 2004.

[30] Dey, A., & Somaiah, S. (2022). Green synthesis and characterization of zinc oxide nanoparticles using leaf extract of Thryallis glauca (Cav.) Kuntze and their role as antioxidant and antibacterial. Microscopy research and technique, 85(8), 2835-2847.

[31] Pathak, J., Akhani, S. B., & Rathore, M. S. (2024). Structural and photoluminescence properties of green synthesized ZnO nanoparticles from Calotropis gigantea leaves. Materials Today: Proceedings.

[32] Tabassam, L., Khan, M. J., Hussain, S., Khattak, S. A., Shah, S. K., & Bhatti, A. S. (2022). Structural, optical and antimicrobial characteristics of ZnO green nanoparticles. Journal of Sol-Gel Science and Technology, 101(2), 401-410.